

ON THE FLUX OF MILLIMETRIC SPACE DEBRIS

R. M. Goldstein
Jet Propulsion Laboratory
California Institute of Technology
Pasadena, CA 91109

S. J. Goldstein, Jr.
Dept. of Astronomy
University of Virginia
Charlottesville, VA 22903

Received _____

Revised _____

ABSTRACT

In 21.4 hours of zenith radar observations on 4 days at 8510 MHz, we found 831 particles with altitudes between 177 and 1662 km. From the duration of the echoes and the angular size (.030 deg) of the antenna beam 158 particles were identified as passing through the side lobes and not through the main beam.

Our analysis is based on the 674 particles that did not broaden the beam. On the assumptions that these particles went through the main beam, their radar cross sections vary between .02 and 260 mm², and their radial velocities vary between ± 700 m/sec. If they are conducting spheres, their diameters lie between 2 and 18 mm. If not, they must be larger. The flux of these particles, that is the number per km² day, was determined in 100 km intervals. The maximum flux, 3.3 particles per km² day, occurs at 950 km altitude.

The small and large particles are not well mixed. The largest particles occur beyond 1000 km and middle-sized particles are missing below 300 km. If the earth's atmosphere caused the smallest particles to lose energy from initial orbits identical to those of the large particles, the orbits would have lower eccentricity at low altitudes. We find a larger eccentricity for the inner particles, and conclude that two or more populations are present.

1. Observations

Space debris is a constantly increasing hazard for operations in space. For objects larger than about 10 cm, the USSPACECOM maintains a catalogue of orbital elements. Their data, obtained with longer wavelength radars, relates to larger scale objects.

Stansbery, et al. (1993) and Kessler (1997+) have used the 3.5 cm Haystack radar to gather statistics on smaller particles of debris. The Haystack radar can detect a 6 mm metallic sphere at a range of 1000 km.

We report here on debris measurements made at the Jet Propulsion Laboratory's Goldstone Observatory. Although the use of this facility for debris monitoring is very limited, the 3.5 cm radar can detect 3 mm conducting spheres at a range of 1000 km. This radar employs a 70 m paraboloid which radiates approximately toward the zenith, and a receiver mounted at the focus of a 35 m paraboloid displaced 497 m from the 70 m antenna. The transmitted power varied between 400 and 466 kw and the measured system noise temperature was between 36 and 37 K on the 4 nights of the observations. Both antennas are nominally directed to a point 1000 km above the midpoint between them. The corresponding shift of each antenna from the zenith is .016 deg, a value smaller than the beam widths, .030 deg for the 70 m telescope, .060 deg for the 35m telescope. Neither antenna is designed to be pointed accurately near the zenith, and the number of observed particles may be diminished near the inner altitude limit by small pointing errors.

The transmitter is on for 1.4 msec while the frequency increases linearly by 46.2 kHz. Then it turns off. There is a 0.2 msec dead time which allows the response from local reflectors in the antenna sidelobes to die out; then the receiver is on for 10.0 msec. The transmitter is on again for 1.4 msec while the frequency decreases linearly by 46.2 kHz. Again there is 0.2 msec of dead time followed by 10.0 msec of the receiver on. The receiver center frequency is constant at 8510 MHz, and each cycle lasts 23.2 msec (more precisely, 23.167 msec).

The receiver provides a baseband signal from the receiving antenna to a 386 computer which also generates the modulating wave for the transmitter. For each receive period, the computer performs a convolution and detection of the received signals with a stored replica of the transmitted chirp. convolution is done with the aid of the fast Fourier transform and a signal processing chip attached to the computer,

Every 69.5 msec three cycles of filtered and detected outputs for both "up-chirp" pulses and "down-chirp" pulses are averaged and transferred to the memory of the host computer. The host computer searches for pairs of pulses greater than 6.5 times the rms noise determined when no pulses are present. This threshold corresponds to an average of one false alarm every 511 hours. When one or more such pairs of pulses are found, the host computer transfers to a permanent file five 69.5 msec pairs centered on the largest pulse.

in Figure 1a we show one such file, where the observed particle has passed through the main beam and in Figure 1b, an observation where the time duration indicates that the particle was observed in the antenna sidelobes.

The measured time delays, as shown in the figure, depend on both the time-of-flight and the Doppler shift of the reflecting object according to

$$\tau_{up} = \tau - f T / F \quad (1)$$

$$\tau_{down} = \tau + f T / F \quad (2)$$

In these equations T is the duration of the transmitted chirp, F is its frequency excursion, τ is the actual time delay of the echo, and f is the Doppler shift. The

time-of-flight is obtained by adding the two equations; the Doppler shift, by subtracting them. For the weakest signals, the accuracy of the time of-flight measurement is the reciprocal of the chirp bandwidth, and for the Doppler measurement it is the reciprocal of the chirp duration. This corresponds to a range uncertainty of 3.2 km and a velocity uncertainty of 12 m/sec. For the stronger signals, the accuracy is much better.

For a particle in circular orbit about the earth, the time to move .030 deg is

$$t = 8.2933 \times 10^{-4} r (r + 6372.0)^{1/2} \quad (3)$$

where t is measured in msec and r is the altitude in km. According to this formula at $r = 977$ km, $t = 69.5$ msec. Thus for altitude less than 977 km, a particle's response is diminished because the averaging process adds observations where the particle was not in the main beam of the antenna.

In the analysis of the next section We use formula (3) with its assumption of a circular orbit to calculate a small correction for the reduction of the radars response to nearby objects, caused by averaging in the data reduction. Some small particles are lost when their response is averaged, and no correction can be made for them.

We note from Table 1 that, in 21.434^h of observing, 831 particles were strong enough to produce both "up" and "down" echoes at least 6.5 time the rms noise; and that 158 of these could be identified as outside the main beam. Formula (3) tells us that at $r = 505$ km, $t = 34.7$ msec or 1/2 the averaging time. At this altitude and below we would not be able to identify a sizeable fraction of particles that did not enter the main beam. In spite of this shortcoming, we now consider all of the observations minus those that took too long to cross the beam, 674 in number.

A second correction has been applied because the two antenna beams are not strictly parallel. They were set to intersect at an altitude of 1000 km, hence at both higher and lower altitudes the observed power is too low. The necessary correction is the reciprocal of the envelope of the smaller antenna's beam.

The measured radar cross sections A can be converted to a diameter on the assumption that the particles are conducting spheres that entered the main beam with the formula

$$D = (A\lambda^4/\pi^5)^{1/6} \quad (4)$$

For a few particles where D exceeds 7.93 mm the formula is

$$D = (4A/\pi)^{1/2} \quad (5)$$

Rayleigh (1888) derived equation (4) for conducting spheres, while equation (5) states that the radar cross section is the geometrical cross section. We regard them as a convenient method for compressing the wide range of A into a more convenient form.

The diameters we report here are a lower limit, for two reasons. First, the particles might not go through the center of the main antenna beam, so that the power is diminished, and second, if the particles are not conducting, they must then be larger to reflect the same power.

Table 2 is a histogram that classifies the observations in altitude and in diameter. Figure 2 gives the calculated diameters for the main beam particles, while Figure 3 gives their radial velocities.

2. Flux of Space Debris Particles

In Table 3 we list for the midpoints of the altitude intervals the area of the region searched by the radar beam. Taking the beam to be circular with .030 deg half-power width we found one dimension of the area from $r = (.030)\pi/180$, while the other is the width of the altitude interval, 100 km. The fluxes listed in Table 3 are, in each size interval, the number of particles divided by the beam area and expressed in units of number per km^2 day. The right hand column is the total particle flux.

The observable diameter range is different in each altitude interval, because of the decreasing sensitivity of the radar with distance. However, the maximum flux at 950 km seems accompanied by lower fluxes at greater and at lower altitudes.

If the distribution of particles were the same in each size interval, we could make

statistical corrections to our sample to evaluate the observational "incompleteness".

This is clearly not the case.

3. A Search for the Evolution of Particle Orbits

In Figure 2 one sees the effect of the finite sensitivity of our instrument in the lower envelope of the plotted points. For the lowest altitudes, the non overlapping of the two antenna beams must also affect the number of particles seen.

The largest particles in Figure 2 and Table 2 do not appear below 1000 km and the intermediate sized particles are absent below 400 km. These latter gaps cannot be observational, but indicate that the relevant particles are too rare to be detected in our 21,4 h observing time, and that the population of particles is not well mixed. Note that the largest particles avoid the regions of both smaller sized particles.

Could it be that all these particles have evolved from a single distribution at large distance, with drag caused by the earth's atmosphere shrinking the orbits of the smaller particles to their present value? See Smart (1953). To answer this question we have applied the least-square method of estimating eccentricity and semi major axis. A particle that obeys all three of Kepler's laws has semi major axis a and eccentricity e that obey the equation

$$a^2(1 - e^2)/r^2 + a(\dot{r}^2/GM - 2/r) - 1 = 0 \quad (6)$$

where r is the particle's radius vector (the altitude plus the radius of the earth), \dot{r} is the radial velocity toward the primary, and GM the geocentric gravitational constant. See (G&G, 1994). We divided the main-beam observations into five groups according to distance in Table 4 and calculated a best-fitting eccentricity and semi major axis for each group. The uncertainties in a and e in Table 4 are calculated as follows: the least-squares values of a and e are perturbed by amounts Δa and Δe such that the residuals are increased by $1/k-2$ where k is the number of observed particles. The closed curve, Δa vs Δe , is plotted and the tangents perpendicular to the Δa axis yield the uncertainty in a while those perpendicular to the Δe axis give the

uncertainties in e . Figure 4 shows the Δa vs Δe curves for all five groups.

A Keplerian particle that receives an impulsive force at pericenter changes both semi major axis a and eccentricity e according to the formula

$$de = \frac{da}{a} (1 - e) \quad (7)$$

In Table 4 we see that decreases in a are not accompanied by decreases in e . For the lowest range interval there seems to be a significant increase in a .

It follows that these orbits did not evolve from a single outer distribution, and that there are at least two distributions present in the space debris.

4- Discussion

The range of observable particles is critically dependent on the modulation pattern and the data reduction scheme used. Thus, our observations do not rule out the existence of more distant particles than 1660 km or less distant particles than 177 km; further particles in orbit about the sun (instead of the earth) would likely have velocities too large to make both up pulses and down pulses simultaneously observable; hence, if they exist, they were excluded by our data reduction.

The existence of multiple populations prevents correcting the observations as Schmidt (1968) corrected the population of quasars. Is the decrease in particle flux beyond 950 km real? From Fig. 2 at a range of 1200 km you can see that numerous particles of 3 mm diameter are observable, but that particles in the range 4 to 8 mm are scarce. Observational selection cannot cause this scarcity, it is real.

Measurements from space or from the ground at lower latitudes can extend our knowledge of space debris to orbits with lower inclination angles. The space debris we have observed at latitude 35.2 deg must have inclination angles equal or greater than 35.2 deg. Our flux values are therefore lower limits to those which occur in the earth's equatorial plane.

Multiple populations tell us that in addition to man-made particles, there may also be natural particles.

Acknowledgement

We thank the staff of the Deep Space Net for their skilled assistance in observing. RMG was supported by Jet Propulsion Lab, California Institute of Technology, under contract with the National Aeronautics and Space Administration. SJG was supported by the University of Virginia, and wishes to thank Dr. Jon Brinkmann for instruction in MSDOS programming.

References

- Goldstein, S. J. and Goldstein, R. M. 1994, *Astron. J.*, 107, 367.
- Kessler, D. J. 1993, *Adv. Spa. Res.* 13, 139.
- Rayleigh, J. 1888, see M. Skolnik "Radar Handbook", McGraw-Hill, 1970, p. 30.
- Schmidt, M. 1968, *Astrophys. J.*, 151, 393.
- Smart, W. M. 1953, "Celestial Mechanics" (Longmans, Green, and Co., London, Ch. 15.
- Stansbery, E. G., Bohannon, G., Tracy, T., and Stanley, J. 1993, *Adv. Spa. Res.* 13, 43.

*Dr R. M. Goldstein**8 pages*

TABLE 1. TIMES OF OBSERVATIONS (UTC)

Date	First Observ.	Last Observ.	Duration (hours)	Total Number	Number in Main Beam	Rate (events/hr)
1993 May 4	9h56m37s	13h49m36s	3.883	131	108	27.8
1993 Jun 11	81011	111653	3.112	83	64	20.6
1993 Dec 22	51636	132452	8.138	350	278	34.2
1994 Mar 26	43153	104957	<u>6.301</u>	<u>267</u>	<u>223</u>	35.4
			21.434	831	673	

TABLE 2, DIAMETER VS. ALTITUDE HISTOGRAM

Midpoint (km)	Number vs diameter (mm)		
	2-4	4-8	8-18
238	17	0	0
350	13	0	0
450	15	1	0
550	40	1	0
650	45	7	0
750	48	14	0
850	66	39	0
950	77	72	0
1050	34	21	2
1150	28	22	2
1250	15	12	2
1350	11	10	2
1450	3	29	3
1550	5	12	2
1650	0	4	0

TABLE 3. PARTICLE FLUX VS DIAMETER

Midpoint (km)	Beam area (km ²)	Number (all sizes)	Flux (num/km ² day)
238	15.36	17	1.24
350	18.33	13	0.80
450	23.56	16	0.76
550	28.80	41	1.60
650	34.03	52	1.71
750	39.27	62	1.77
850	44.51	105	2.65
950	49.74	149	3.36
1050	54.98	57	1.16
1150	60.21	52	0.97
1250	65.45	29	0.50
1350	70.69	23	0.36
1450	75.92	35	0.52
1550	81.16	19	0.26
1650	86.39	4	0.05

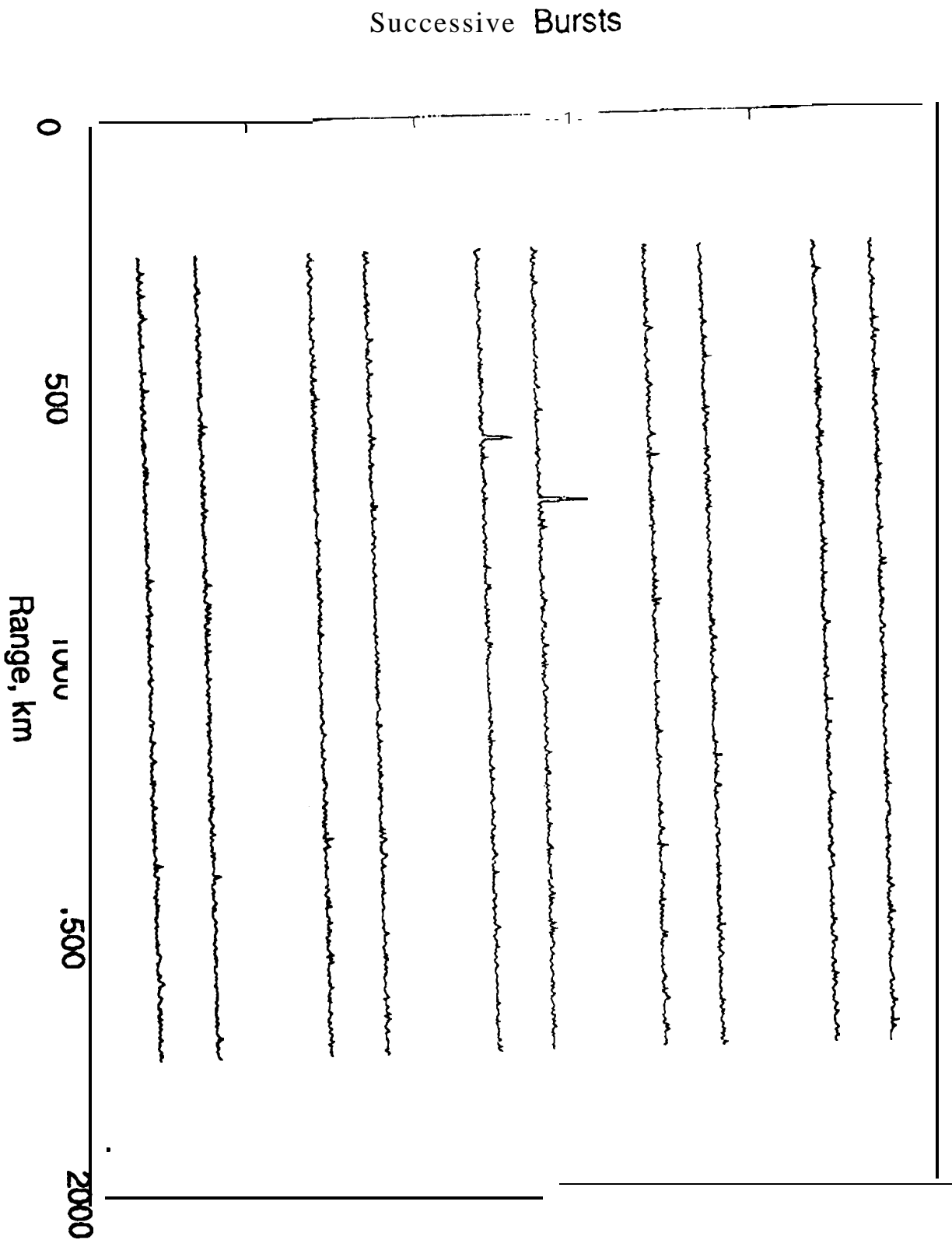
TABLE 4. LEAST-SQUARE SEMI-MAJOR AXES AND ECCENTRICITIES FOR VARIOUS ALTITUDE RANGES

Altitude Range (km)	Number of Particles	a (km)	e
177-500	46	6823 ⁺¹⁴⁰ ₋₁₂₀	.0511 ^{+.0085} _{-.0062}
500-700	93	6917 ⁺¹²⁰ ₋₁₃₀	.0299 ^{+.0110} _{-.0062}
700-1100	373	7276 ⁺⁷⁰ ₋₇₀	.0230 ^{+.0048} _{-.0060}
1100-1400	104	7587 ⁺¹⁶⁰ ₋₁₄₀	.0273 ^{+.0082} _{-.0098}
1400-1662	58	7937 ⁺⁴⁵⁰ ₋₄₄₀	.0309 ^{+.0381} _{-.0179}

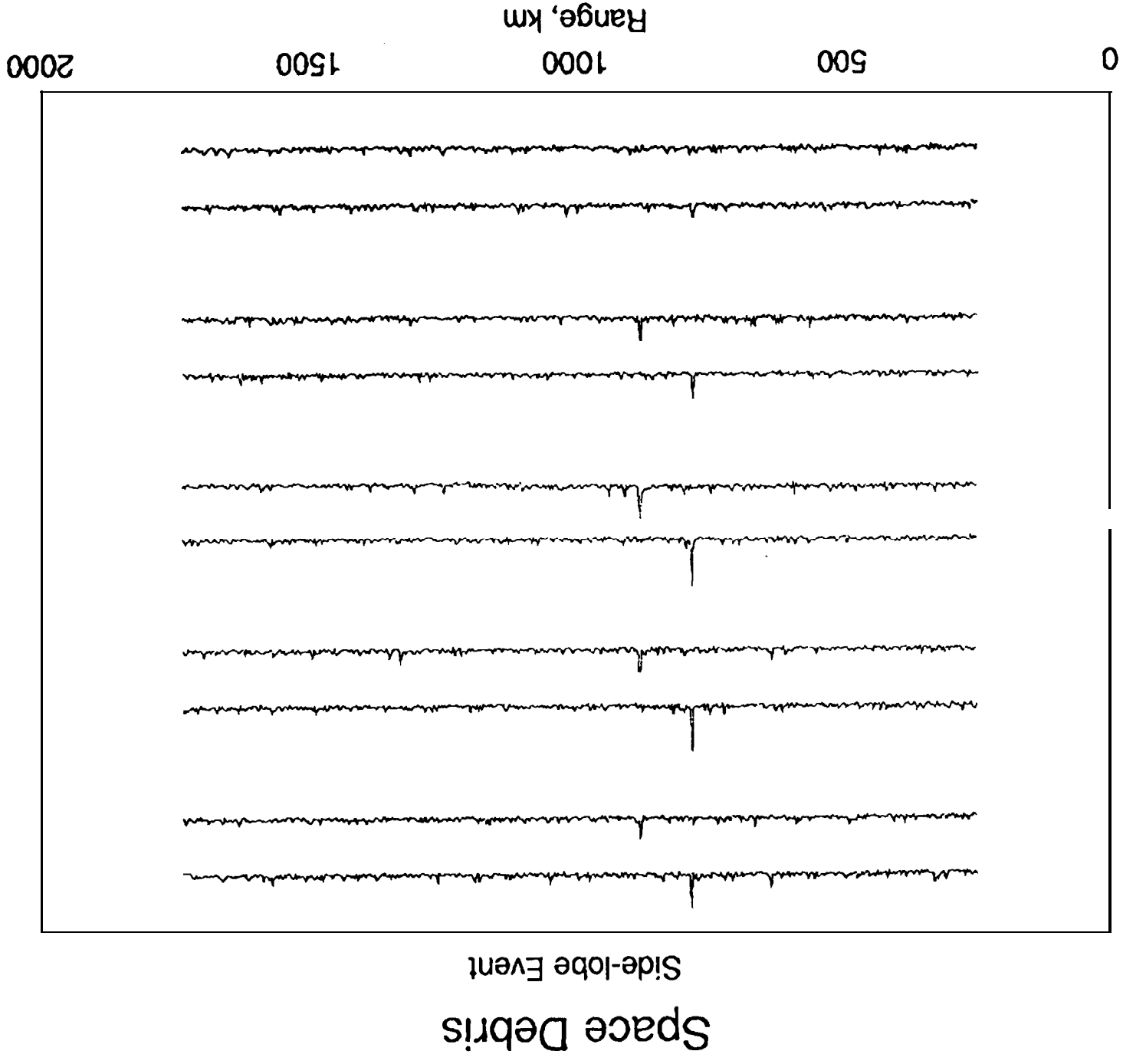
TABLE 4. LEAST SQUARE SEMI-MAJOR AXES AND ECCENTRICITIES FOR VARIOUS ALTITUDE RANGES

Altitude Range (km)	Number of Particles	a (km)	e
177-500	46	6823^{+140}_{-120}	$.0511^{+.0085}_{-.0062}$
500-700	93	6917^{+120}_{-130}	$.0299^{+.0110}_{-.0062}$
700-1100	373	7276^{+70}_{-70}	$.0230^{+.0048}_{-.0060}$
1100-1400	104	7587^{+160}_{-140}	$.0273^{+.0082}_{-.0098}$
1400-1662	58	7937^{+450}_{-440}	$.0309^{+.0381}_{-.0179}$

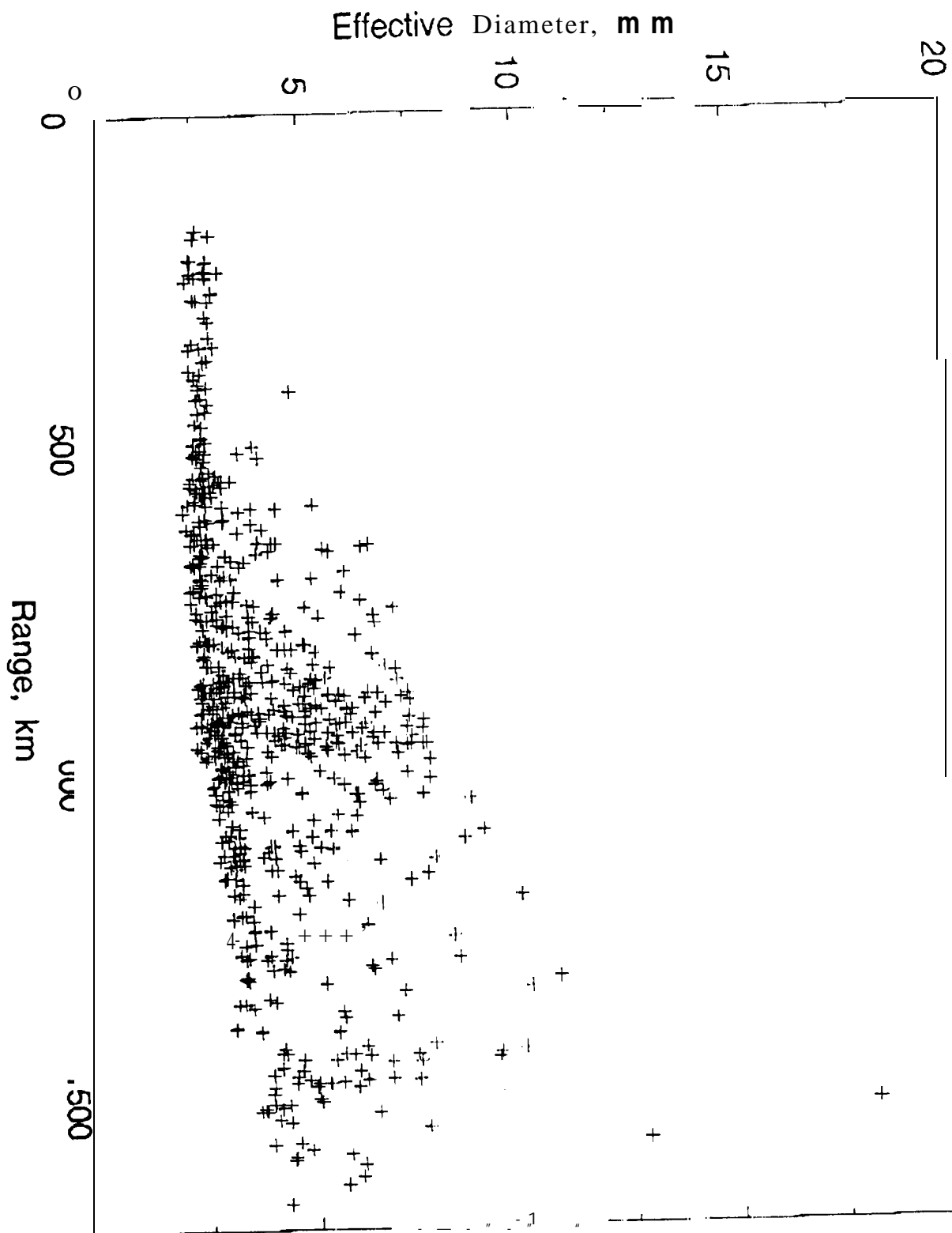
Space Debris Main Beam Event



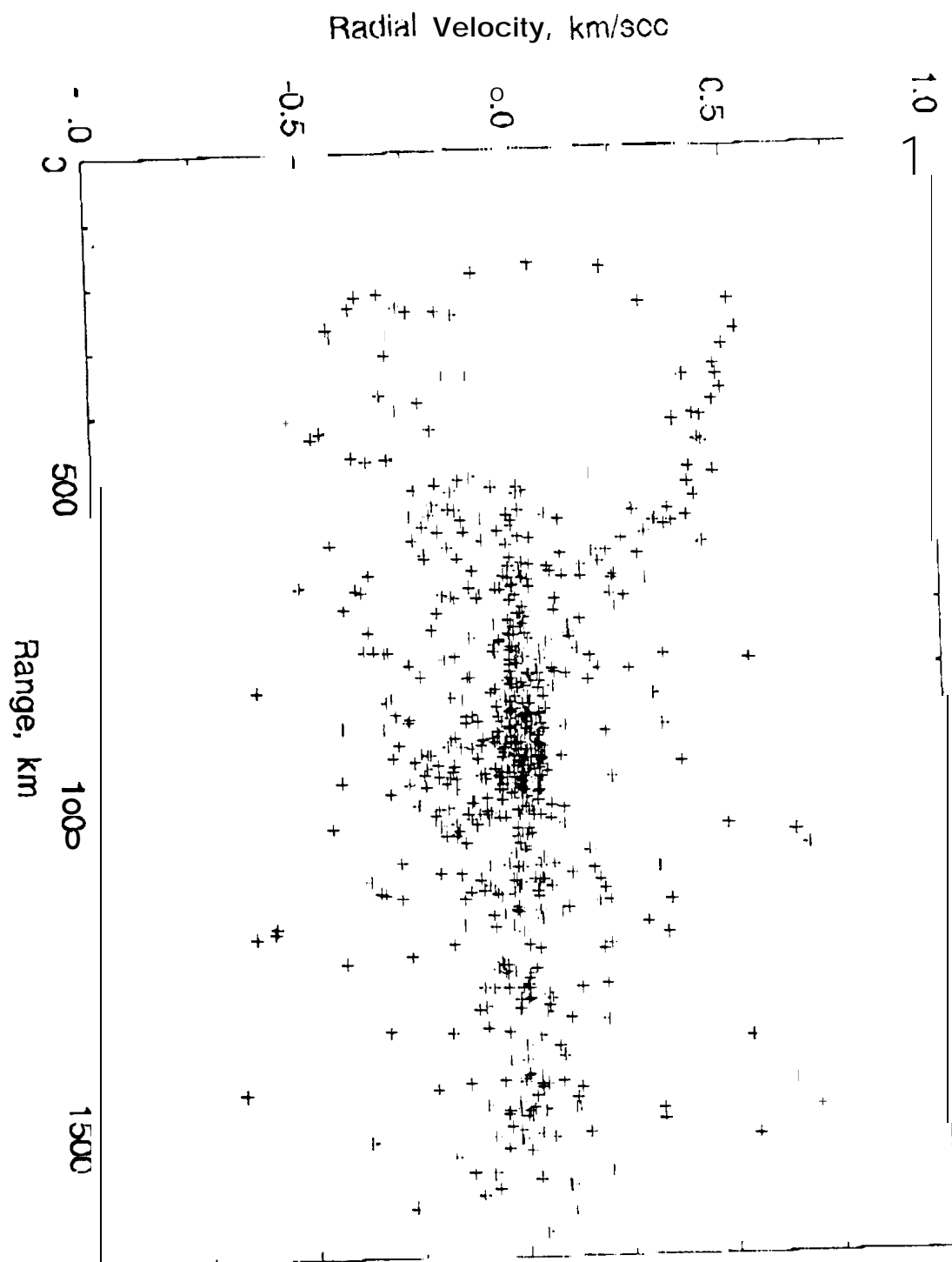
Successive Bursts



Space Debris



Space Debris



01
02
03
04
05
06

ECCENTRICITY

